

Lift Enhancement of a Vortex-Sink Attached to a Flat Plate

X. XIA¹, AND J. MULLEN[†], AND K. MOHSENI^{1,2} ‡,

¹Department of Mechanical and Aerospace Engineering, University of Florida, Gainesville, FL, 32611-6250, USA

²Department of Electrical and Computer Engineering, University of Florida, Gainesville, FL, 32611-6250, USA.

(Received ?? and in revised form ??)

As observed in natural fliers, stabilized vortices on the surface of an airfoil or wing could provide lift enhancement. Similar concept can be applied in fixed lifting surfaces. Potential flow theory is employed to model lift enhancement by attaching a vortex-sink pair to the top surface of a flat plate in a pseudo-steady flow. Using this flow model, a parametric study on the location of the vortex-sink pair is performed in order to optimize lift enhancement. Lift coefficient calculations are presented for a range of vortex-sink positions, vortex-sink strengths, and flat-plate angles of attack. It is shown that beyond the lift contribution terms due to the vortex-sink strength, lift enhancement could be also achieved by a translating velocity of the vortex-sink in a non-equilibrium position. This vortex-sink velocity term is more pronounced when the vortex-sink is placed close to the top surface of the flat-plate near the leading or the trailing edges of the flat plate. It is concluded that increasing the vortex strength and placing the vortex-sink near the surface of the flat plate are the two most effective ways of enhancing lift. Furthermore, understanding of the translational vortex-sink velocity lift contribution term might inspire new control strategies, such as vortex-sink velocity manipulation, in future lift enhancement applications.

Key words: Attached vortex-sink, potential flow, lift coefficient.

1. Introduction

Insects have demonstrated the capacity for high performance hovering flight with unrivaled maneuverability and speed. Over the last several decades, scientists have tried to understand and explain the unsteady aerodynamic principles that account for such flight characteristics. This high performance has been attributed to, among other things, an attached leading edge vortex (LEV) which induces a dynamic stall condition at high angles of attack, providing lift enhancement (Ellington 1984; Dickinson & Gotz 1993).

LEVs naturally occur in flapping flight which provides aerodynamic advantages. The first theoretical evidence for lift enhancement in an attached free vortex over a flat plate was offered by Saffman & Sheffield (1977). They considered a steady two-dimensional irrotational flow over a wing with an attached free line vortex. In their model, the presence of a vortex results in increased lift. Following this research, Huang & Chow (1981) extended Saffman and Sheffield's work to include the effects of airfoil thickness and camber.

[†] Current address Boeing Company Seattle, Washington

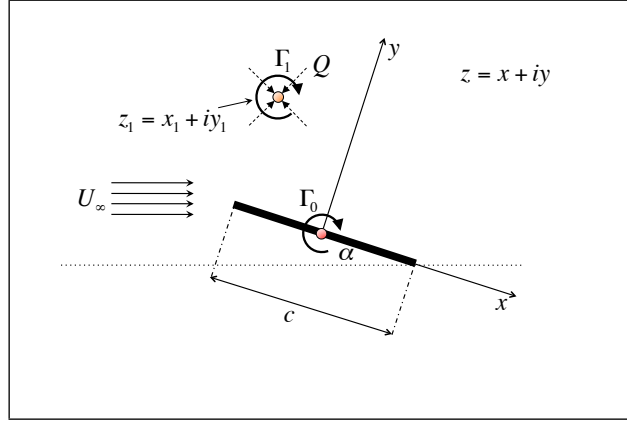
[‡] Email address for correspondence: mohseni@ufl.edu

Similar to Saffman and Sheffield's approach, Rossow (1978) used an airfoil in his model instead of a flat plate, while adding a nose flap to trap a vortex. To represent the model for observed vorticity bleeding from the LEV by span-wise flow, he also added a sink at the vortex core which inspired further investigations by Mourtos & Brooks (1996). The first physical experiments, verifying the models' result that the LEV provides lift enhancement, was performed by Ellington (1984). All this preliminary research pointed to the same conclusion: attaching and stabilizing a vortex on the upper side of an airfoil will increase the lift coefficient.

Moreover, over the last decade, many studies of aerodynamic forces in insects have indicated that a significant part of lift production is generated during the translational phases of the stroke (upstroke and downstroke); see Willmott *et al.* (1997). For flapping fliers, the LEV appears attached to the wing throughout the translation phase of flapping (Birch & Dickinson 2001). The prominent theory of LEV stabilization has been attributed to a span-wise flow that bleeds excess vorticity from the vortex core, preventing it from growing in strength and shedding. This phenomena was verified in a three-dimensional computational study of the hawkmoth (Lia *et al.* 1998). Furthermore, Birch & Dickinson (2001) and Swanton, Vanier, and Mohseni (Swanton *et al.* 2008) experimentally showed that the LEV becomes unstable if the span-wise flow is blocked, implying that the span-wise flow might be a necessary mechanism to stabilize the vortex.

An implicit assumptions in these investigation was that the free trapped vortex is somehow stabilized over the lifting surface. To this end, several studies assumed that the vortex should be located at the equilibrium point in the flow and then they studied the stability of these equilibrium points; see Saffman & Sheffield (1977); Rossow (1978); Huang & Chow (1981, 1996); Mourtos & Brooks (1996). In this study we will revisit these assumptions for a two dimensional quasi-steady flow over a lifting surface with a trapped vortex-sink pairs. Here, it is further assumed that even in cases that the equilibrium points are not stable, flow augmentation methods and control laws have matured to the point where a vortex may be placed anywhere around the surface of a flat plate, at least over a limited period. Several flow augmentation devices, investigated for separation bubble control, include synthetic jets (Lopez *et al.* 2009; Muse *et al.* 2008; Krishnan & Mohseni 2009*a,b*), flaps (Kasper 1974), and air jets (Cornish 1969). With such advancements, one could hope for future design of more efficient and highly maneuverable fixed, flapping, and flexible aerial vehicles; particularly in low Reynolds number flow regimes. To achieve that an interesting question rises: if a vortex could be placed anywhere over an airfoil, what location could provide the maximum lift enhancement?

In this investigation, with the span-wise flow represented by a sink at the vortex center, a two-dimensional steady potential flow model is presented to determine the location of a vortex-sink pair for maximized lift generation. Moreover, parametric studies are performed in order to determine the effect of various flow parameters on the lift coefficient. It should not be ignored that there are already previous research about vortices dynamics and force calculation of vortices and rigid body systems using unsteady potential flow techniques (Cortelezzi & Leonard 1993; Crowdy 2010; Kanso & Oskoueï 2008; Clements 1973; Smith 2011; Michelin & Smith 2009). While most of these studies were focused on vortices dynamics and shedding without calculating the lift generated, Michelin & Smith (2009) systematically went through the force calculation and the dynamics of the coupled fluid-solid system. Despite the more accuracy in predicting the vortex shedding behaviors and unsteady force calculations, this study were introducing multi-vortices or vortices sheet into the system which required numerically solving for non-linear ODE systems. This would add extra complexity to solving the problem itself and result in the lift expression being implicit. In this sense, we are in the direction of implementing a

FIGURE 1. z coordinate frame. Flow over a flat plate of length $c = 4a$.

simple model with only one vortex-sink to represent the vortices system and computing the lift explicitly. In this way, we are able to obtain relatively concise expression of the lift and identify different contributions of lift. Furthermore, this lift computation enables us to relate the location and velocity of the leading edge vortex directly to the lift generated which would be helpful for future active flow control applications. We believe that this lift computation provide adequate accuracy for flow control as it is improved based on the classical Kutta-Joukowski lift theorem. The analysis presented in this study ignores the unsteady flow and viscous effects. The impact of these effects will be the subject of a future investigation.

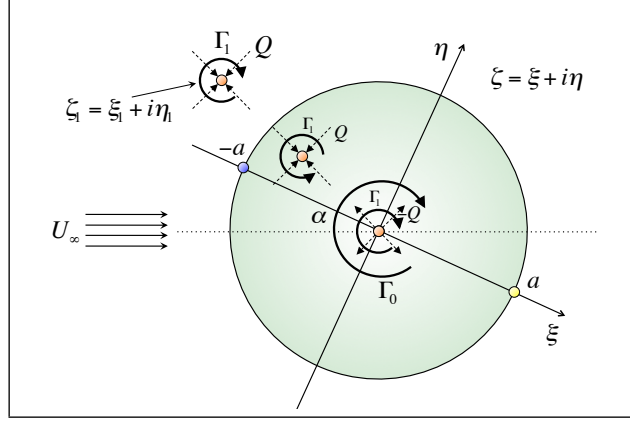
This paper is organized as follows: Section 2 provides the derivation of the potential flow model around a flat plate with an attached vortex and sink. Section 3 discusses the aerodynamics of a vortex-sink attached to a flat plate. Section 4 presents the lift enhancement optimization results. Section 5 discusses the unsteady issues. Finally, concluding remarks are presented in Section 6.

2. Flow Model

2.1. 2-D Potential Flow Derivation

While our motivation comes from flapping, here we start with a simplified case: a flat plate with a vortex attached. It is assumed that the vortex has been generated already by means of flapping or some sort of flow augmentation. Therefore, the free stream velocity has no component due to flapping, it is simply the speed at which the object is moving through the flow at infinity. The mathematical model presented here assumes the flow is two-dimensional, inviscid, and irrotational; therefore, in the the governing equations the Laplacian of the complex potential vanishes and the superposition principle implies that vortex singularities may be added together in order to satisfy the boundary conditions and to generate the flow field. The flow around a flat plate (see Figure 1) is obtained by the application of the Joukowski transformation to the flow over a cylinder (see Figure 2). The trapped vortex is presented by an attached line vortex and the span-wise flow is modeled by a sink co-located with the vortex.

Writing out the complex potential for the flow around a cylinder with an attached

FIGURE 2. ζ coordinate frame. Flow over a cylinder of radius a .

vortex-sink results in the following equation:

$$w(\zeta) = U_\infty \left[e^{-i\alpha} \zeta + \frac{a^2 e^{i\alpha}}{\zeta} \right] + \frac{1}{2\pi} \left[[i(\Gamma_0 + \Gamma_1) - Q] \ln(\zeta) + (Q + i\Gamma_1) \ln(\zeta - \zeta_1) + (Q - i\Gamma_1) \ln\left(\zeta - \frac{a^2}{\zeta_1}\right) \right], \quad (2.1)$$

where U_∞ is the flow at infinity, α is the angle of attack, Γ_1 is the strength of the attached external vortex, Γ_0 is the strength of the additional central vortex introduced in order to satisfy the Kutta condition (see section 3.2), Q is the strength of the sink, and a is the radius of the cylinder. In order to preserve the shape of the cylinder, a set of two image vortices and sinks have been introduced inside the cylinder in accordance with the circle theorem (Milne-Thomson 1958). One may use the Joukowski transformation to map out the flow over a cylinder into the flow around a flat plate as given by:

$$z = \zeta + \frac{a^2}{\zeta}. \quad (2.2)$$

A similar potential flow model has been used by others including Huang & Chow (1981) and Mourtos & Brooks (1996). An example of streamlines generated in such a flow is shown in Figure 3. The line connecting the vortex-sink to the outside boundary is a branch-cut as discussed below.

The stream function is obtained by taking the imaginary component of the complex potential shown in Equation (2.1). This stream function has two properties of interest to our study: contour plots of the stream function are the streamlines and the difference in value of the stream function between two points represent the total flow between the points. If the flow includes a source or sink, the complex potential function will be analytic, using the proper Riemann surface. However, to accommodate for the mass transfer out of the sink, the stream function will have branch-cuts with a specified jump along a rather arbitrary line connecting the source or sink to infinity (Ablowitz & Fokas 2003). This branch cut guarantees that integrating the stream function along a closed path including the source will result in the exact flow rate out of the source or sink. Because this is a two-dimensional flow, the mass flow rate must come from infinity through the branch cuts as shown in Figure 3. In this flow model, there are three branch cuts accounting for the three sinks/sources shown in Figure 2.

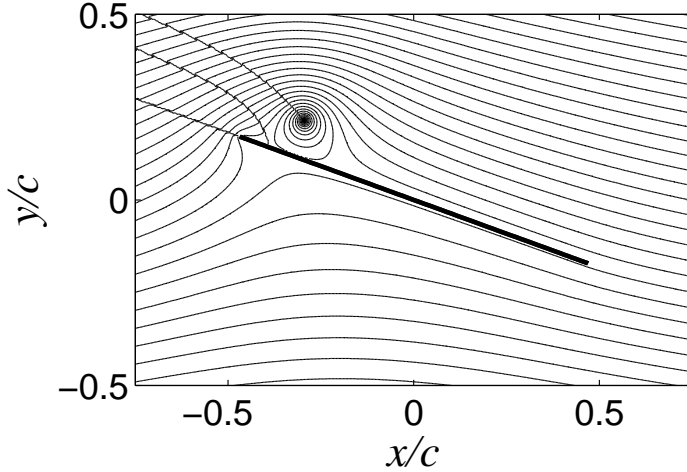


FIGURE 3. Sample streamlines for a flow over a flat plate with an attached vortex-sink. The lines connecting the center of the vortex-sink to the far field are arbitrary branch-cuts.

2.2. Nondimensionalization

As shown in Figure 1, the computational domain is a flat plate at an angle of attack α with respect to a free stream flow with velocity U_∞ . The external vortex of strength Γ_1 and sink of strength Q are located at point (x_1, y_1) with respect to the flat plate's frame of reference. Other parameters involved in this flow are the fluid density, ρ , the chord length of the flat plate, c , and the lift per unit depth, L . An application of the Buckingham Π theorem results in a set of five non-dimensional numbers $(\frac{x_1}{c}, \frac{y_1}{c}, \frac{\Gamma_1}{cU_\infty}, \frac{Q}{cU_\infty}, \alpha)$ which govern the flow and the sectional lift coefficient $C_l = \frac{L}{\frac{1}{2}\rho U_\infty^2 c}$. All of the results in the following sections are presented in terms of these non-dimensional numbers.

3. Aerodynamics of Attached Vortex-Sink

3.1. Lift Computation

There has been very little research into the effect of a vortex-sink pair on the aerodynamics of airfoils. Previous research that modeled a vortex-sink at its equilibrium location utilized the simplified version of the Blasius Theorem by directly applying the Kutta-Joukowski theorem to compute the lift (Mourtos & Brooks 1996; Rossow 1978)

$$L = \rho \Gamma U_\infty. \quad (3.1)$$

However, in this study the vortex-sink is not limited to the equilibrium location, and application of Equation (3.1) to compute the lift for the flow described by Equation (2.1) is inadequate because it ignores the effect of the singular point due to the presence of a vortex-sink pair. Therefore, in order to compute the coefficient of lift of the flat plate under quasi-steady-state assumption, the Blasius theorem (Milne-Thomson 1958) will be utilized. This theorem is used to compute and estimate the forces on a two-dimensional body by the following integral:

$$D_z - iL_z = \frac{i}{2}\rho \oint_{C_1} \left(\frac{dw}{dz} \right)^2 dz, \quad (3.2)$$

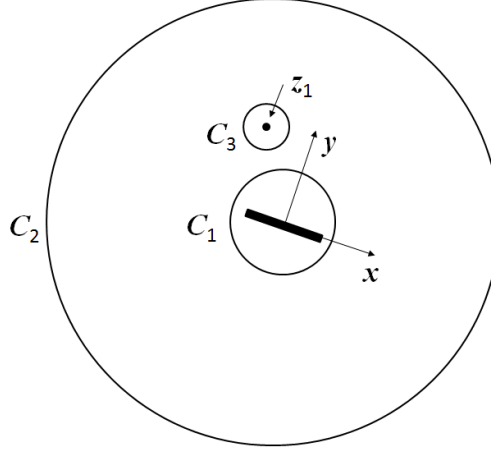


FIGURE 4. Integration contours C_1, C_2, C_3 for Blasius Theorem: C_1 only contains the flat plate, C_2 is at the infinity and encloses all, C_3 only contains vortex-sink.

where L_z and D_z are the lift and drag forces in the z -plane, respectively. As shown in Figure 4, C_1 should be a contour around the flat plate that excludes any singular points (the vortex-sink pair in this case). In order to solve Equation (3.2), we create a large contour C_2 at infinity that includes both the flat plate and the vortex-sink pair at z_1 in z -plane, and another small contour C_3 only including the singular point. As $(\frac{dw}{dz})^2$ is analytic inside the region $C_2 - C_1 - C_3$, we obtain

$$\oint_{C_1} \left(\frac{dw}{dz}\right)^2 dz = \oint_{C_2} \left(\frac{dw}{dz}\right)^2 dz - \oint_{C_3} \left(\frac{dw}{dz}\right)^2 dz, \quad (3.3)$$

This integral is further evaluated in the following sections.

3.1.1. Integration at the Far Field

Here we first compute the integral at infinity. For a Joukowski transformation described in Equation (2.2), we have the following relations as z approximate infinity (Milne-Thomson 1958):

$$\zeta = z \text{ as } |z| \rightarrow \infty, \quad (3.4a)$$

$$\frac{d\zeta}{dz} = 1 \text{ as } |z| \rightarrow \infty. \quad (3.4b)$$

Combined with Equation (2.1), we take the derivative of the velocity potential at infinity, $w_\infty(z)$, yields,

$$\frac{dw_\infty(z)}{dz} = U_\infty e^{-i\alpha} + \frac{i(\Gamma_0 + \Gamma_1) + Q}{2\pi z} - \frac{a^2 e^{i\alpha}}{z^2}. \quad (3.5)$$

Now, applying Cauchy's residue theorem around contour C_2 , we obtain,

$$\oint_{C_2} \left(\frac{dw}{dz}\right)^2 dz = \oint_{C_2} \left(\frac{dw_\infty(z)}{dz}\right)^2 dz = 2\pi i \left\{ \frac{U_\infty e^{-i\alpha} [Q + i(\Gamma_0 + \Gamma_1)]}{\pi} \right\}. \quad (3.6)$$

Next, the second term on the right hand side of Equation (3.3) is evaluated.

3.1.2. The Singular Point

As ζ_1 is a singular point in ζ -plane, it is implied that the corresponding z_1 is also a singular point in the transformed z -plane. In order to calculate the integral around the

contour C_3 , we divide the velocity potential into two parts:

$$w(z) = w'(z) + \frac{Q + i\Gamma_1}{2\pi} \ln(z - z_1). \quad (3.7)$$

Here, $w'(z)$ represents the velocity potential that excludes the contribution from the vortex-sink, and is therefore analytic over the region surrounded by contour C_3 . Taking the derivative of $w(z)$ in Equation (3.7) yields

$$\frac{dw(z)}{dz} = \frac{dw'(z)}{dz} + \frac{Q + i\Gamma_1}{2\pi(z - z_1)}. \quad (3.8)$$

Taking the square of both sides, we obtain

$$\left(\frac{dw(z)}{dz}\right)^2 = \left(\frac{dw'(z)}{dz}\right)^2 + \frac{Q + i\Gamma_1}{\pi} \frac{dw'(z)}{dz} \frac{1}{z - z_1} + \frac{(Q + i\Gamma_1)^2}{4\pi^2} \frac{1}{(z - z_1)^2}. \quad (3.9)$$

As discussed above, since $w'(z)$ is analytic inside contour C_3 it follows that $\frac{dw'(z)}{dz}$ and $\left(\frac{dw'(z)}{dz}\right)^2$ are also analytic inside C_3 . Therefore, the integral around C_3 can be computed with Equation (3.9) using Cauchy's residue theorem,

$$\oint_{C_3} \left(\frac{dw}{dz}\right)^2 dz = 2\pi i \left\{ \frac{Q + i\Gamma_1}{\pi} \left(\frac{dw'(z)}{dz}\right) \Big|_{z=z_1} \right\}, \quad (3.10)$$

where the extra term $\left(\frac{dw'(z)}{dz}\right) \Big|_{z=z_1}$ needs further calculation. From the Joukowski transformation, as $\zeta \rightarrow \zeta_1$, $z \rightarrow z_1$, so we can compute the following approximation of Equation (3.7) at the singular point

$$\begin{aligned} & \left(\frac{dw'(z)}{dz}\right) \Big|_{z=z_1} \\ &= \lim_{\zeta \rightarrow \zeta_1} \frac{d}{dz} \left[w(z(\zeta)) - \frac{Q + i\Gamma_1}{2\pi} \ln(\zeta - \zeta_1) + \frac{Q + i\Gamma_1}{2\pi} \ln\left(\frac{\zeta - \zeta_1}{z - z_1}\right) \right]. \end{aligned} \quad (3.11)$$

With some algebra,

$$\begin{aligned} & \left(\frac{dw'(z)}{dz}\right) \Big|_{z=z_1} \\ &= \frac{\zeta_1^2}{\zeta_1^2 - a^2} \left[U_\infty \left(e^{-i\alpha} - \frac{a^2 e^{i\alpha}}{\zeta_1^2} \right) + \frac{1}{2\pi} \frac{i(\Gamma_0 + \Gamma_1) - Q}{\zeta_1} + \frac{1}{2\pi} \frac{Q - i\Gamma_1}{\zeta_1 - \frac{a^2}{\zeta_1}} \right] \\ & \quad - \frac{Q + i\Gamma_1}{\pi} \frac{\zeta_1 a^2}{(a^2 - \zeta_1^2)^2}. \end{aligned} \quad (3.12)$$

Therefore, the integral around C_3 can be computed from Equation (3.10) and Equation (3.12). Here, it is important to identify the $\left(\frac{dw'(z)}{dz}\right) \Big|_{z=z_1}$ as the desingularized complex velocity of the background flow at the location of the vortex-sink, in which the last term is known as Routh correction (Lin 1941; Clements 1973). According to Kirchhoff's equation, the velocity of the vortex equals to the desingularized background flow which could be expressed as:

$$u_{vs} - iv_{vs} = \left(\frac{dw'(z)}{dz}\right) \Big|_{z=z_1}. \quad (3.13)$$

where $u_{vs} - iv_{vs}$ is the conjugate of the vortex-sink velocity.

3.1.3. Lift Expression

Now, the expression for lift & drag in the z -plane is finalized as:

$$D_z - iL_z = \underbrace{-\rho U_\infty e^{-i\alpha} [Q + i(\Gamma_0 + \Gamma_1)]}_{\text{Kutta-Joukowski term}} + \underbrace{\rho(Q + i\Gamma_1)(u_{vs} - iv_{vs})}_{\text{Vortex-sink velocity term}}, \quad (3.14)$$

with $u_{vs} - iv_{vs}$ given by Equation (3.12) and Equation (3.13). Consequently, the real lift according to the direction of incoming flow U_∞ could be obtained by the following transformation:

$$L = L_z \cos\alpha - D_z \sin\alpha. \quad (3.15)$$

Next, we will show that this lift expression matches previous lift computations. For the case that there are no singularities in the flow (thus, $Q = 0$ and $\Gamma_1 = 0$) at zero angle of attack, the common expression of lift as derived by the Kutta-Joukowski theorem (Kuethe & Chow 1998) is obtained. Moreover, we take one more step to verify the cases where there is a vortex-sink pair at the equilibrium location ($Q \neq 0$) as provided in Mourtos & Brooks (1996) and Rossow (1978). Here, to satisfy the condition of equilibrium, the vortex-sink velocity, $u_{vs} - iv_{vs}$, is set to be zero in Equation (3.14) and the lift & drag in this case becomes,

$$D_z - iL_z = -\rho U_\infty e^{-i\alpha} [Q + i(\Gamma_0 + \Gamma_1)], \quad (3.16)$$

where L_z and D_z are computed to be

$$L_z = \rho U_\infty [(\Gamma_0 + \Gamma_1) \cos\alpha - Q \sin\alpha], \quad (3.17a)$$

$$D_z = \rho U_\infty [-(\Gamma_0 + \Gamma_1) \sin\alpha - Q \cos\alpha]. \quad (3.17b)$$

Replacing L_z and D_z in Equation (3.15) yields,

$$L = \rho U_\infty (\Gamma_0 + \Gamma_1). \quad (3.18)$$

This matches the simple lift computation equation used in previous studies (Mourtos & Brooks (1996) and Rossow (1978)).

Finally, it should be noticed that in Equation (3.14), the lift & drag are determined by two terms, namely the Kutta-Joukowski term and the vortex-sink velocity term. Obviously, the Kutta-Joukowski term is the basic term that emerges in all lift calculations, while the vortex-sink velocity term is an extra term that is caused by the existence of the vortex-sink. Therefore, it is reasonable to speculate that the natural lift enhancement brought by vortex-sink is related to this vortex-sink velocity term and proper manipulation of the vortex-sink velocity might be helpful in future lift control applications. In later sections, the lift will be evaluated for different cases and the role played by the vortex-sink velocity in lift enhancement will be discussed.

3.2. Kutta Condition

Since viscous effects are ignored in a potential flow model, the Kutta condition simply states that all the viscous effects can be incorporated into a single edge condition (Crighton 1985) which allows the Blasius theorem to be applied to compute the aerodynamic forces. A common way of describing the Kutta condition for steady flows is known as the steady state trailing edge Kutta condition which states such that there should be a finite velocity at the trailing edge (Saffman & Sheffield 1977; Huang & Chow 1981; Mourtos & Brooks 1996). Therefore, after some algebra, the steady state Kutta condition simply places a stagnation point at the trailing edge in the ζ -plane and it must be satisfied for all time. By applying this condition, one can obtain an estimate of the induced circulation, Γ_0 , around the flat plate and consequently the aerodynamic forces.

Mathematically, this condition is implemented by placing a stagnation point at the trailing edge of the cylinder in the ζ -plane so that a finite velocity at the trailing edge of the flat plate in the z -plane is guaranteed. Thus the velocity at the upper and lower surfaces of the plate at the trailing edge will be equal, which implies the streamline emanating from this stagnation point will be parallel to the plate, fulfilling the condition proposed by Chen & Ho (1987); Poling & Telionis (1987). By satisfying this Kutta condition, the bound vortex strength Γ_0 is calculated to be

$$\Gamma_0 = 2a \left[2\pi U_\infty \sin(\alpha) + \frac{\Gamma_1(\xi_1 - a) - Q\eta_1}{a^2 - 2a\xi_1 + \xi_1^2 + \eta_1^2} \right]. \quad (3.19)$$

It is important to note that a real flow with a vortex attached to a flat plate could be highly unstable and unsteady; however, the complexity of implementing unsteady Kutta conditions would add more difficulty to our problem. Therefore, in order to simplify the model for this investigation, it is assumed that the airfoil is a flat plate, not rotating, and the attached vortex is stabilized so that the flow is quasi-steady. The unsteady effect, however, should not be ignored and it will be discussed in the last section in this paper.

4. Lift Enhancement and Optimization

This parametric study examines how the coefficient of lift changes as a function of position of the vortex-sink, vortex strength, sink strength, and angle of attack. With this analysis, we are trying to find the locations for maximized lift enhancement and how the lift is affected by the other parameters.

4.1. Optimization of Vortex-sink Location (x/c , y/c)

Figure 5 shows the contours of lift coefficient vs. vortex-sink location for several cases. It is apparent that regardless of the differences in vortex strength, sink strength or angle of attack, the enhanced lift always occurs when the vortex sink is placed in the vicinity of the leading or trailing edge; in addition, the lift is magnified as the vortex-sink approaches the surface of the plate. This data is presented in more detail in Figure 6, which shows the lift contours for a given y_1/c value plotted against streamwise location x_1/c for increasing angles of attack. It is clear that significant lift enhancement occurs at both the leading and trailing edge, although the latter case demonstrates a greater increase and larger region of influence. Similar to Figure 5, the lift in both regions is seen to increase as the vortex sink is brought closer to the surface of the plate. It is interesting to note that these trends do not vary with angle of attack. In summary, understanding the trends due to vortex-sink location will be important for optimizing the placement of the vortex-sink in flow control.

This can be explained by the lift computation given in Equations (3.12) and (3.14). As the vortex-sink approaches the flat plate surface, the $\zeta_1 - \frac{a^2}{\zeta_1}$ term in Equation (3.12) approaches zero which results in a larger vortex-sink velocity in Equation (3.14) and eventually causes enhanced lift. Actually, the term $\zeta_1 - \frac{a^2}{\zeta_1}$ could be interpreted as the interaction between the vortex-sink and the image vortex-sink representing the effect of the airfoil wall. As the vortex-sink comes closer to the flat plate surface, their interaction becomes stronger which induces a larger vortex-sink velocity while also generating an enhanced lift on the flat plate. Moreover, as the vortex-sink approaches the leading edge or the trailing edge, both the $\zeta_1^2 - a^2$ and $\zeta_1 - \frac{a^2}{\zeta_1}$ terms approach zero. This increases the velocity term in Equation (3.14) which results in peak lift coefficient at the leading and trailing edges. The physical explanation for this is that when the vortex-sink ap-

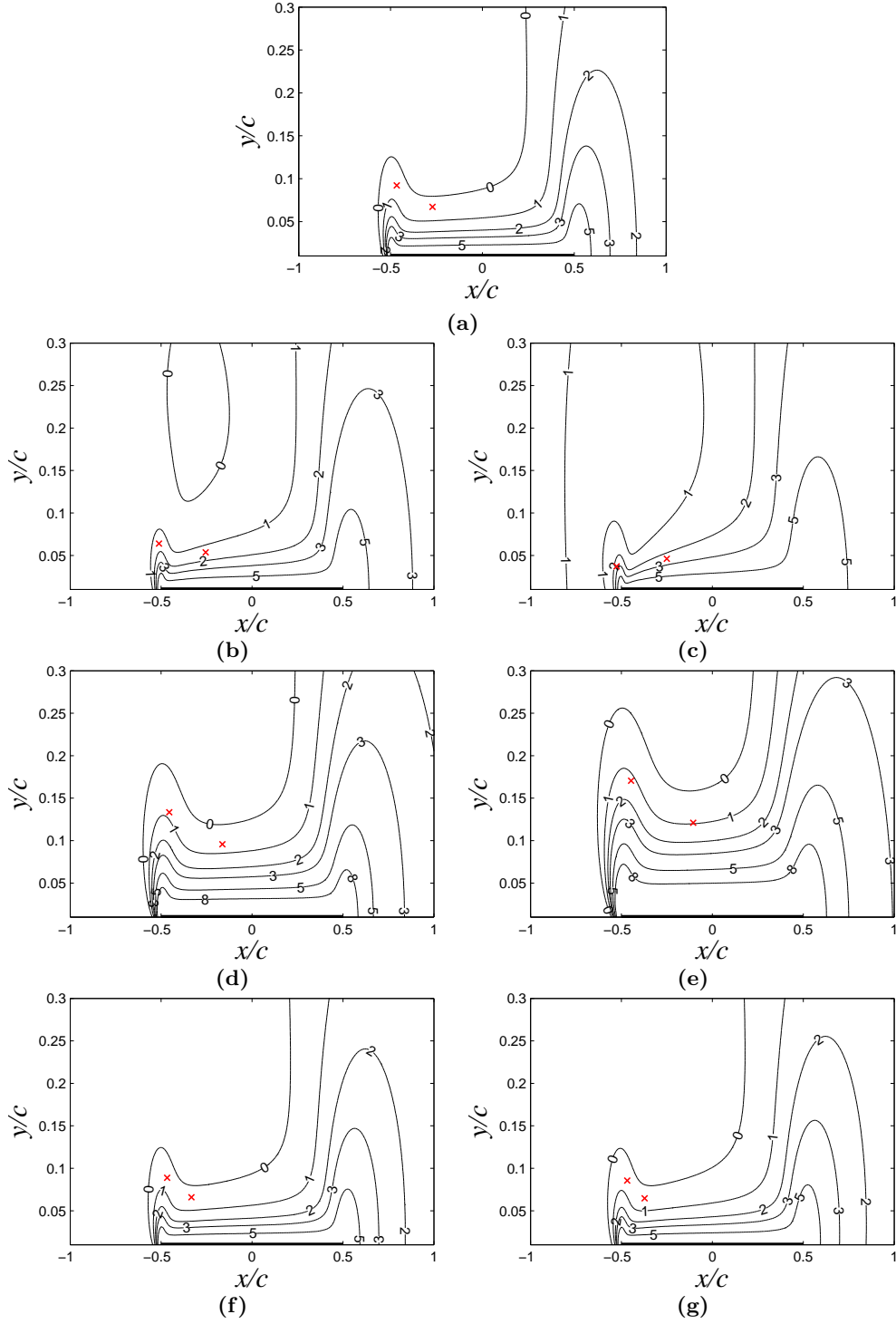


FIGURE 5. Lift coefficient, C_l , contours for varying angles of attack (a,b,c), vortex strengths (a,d,e) and sink strengths (a,f,g). The red crosses represent the locations of two equilibrium points (discussed in the next subsection). (a) Baseline case: $\Gamma_1/cU_\infty = 1.0$, $Q/cU_\infty = -0.1$, $\alpha = 0^\circ$; (b) $\Gamma_1/cU_\infty = 1.0$, $Q/cU_\infty = -0.1$, $\alpha = 10^\circ$; (c) $\Gamma_1/cU_\infty = 1.0$, $Q/cU_\infty = -0.1$, $\alpha = 20^\circ$; (d) $\Gamma_1/cU_\infty = 1.5$, $Q/cU_\infty = -0.1$, $\alpha = 0^\circ$; (e) $\Gamma_1/cU_\infty = 2.0$, $Q/cU_\infty = -0.1$, $\alpha = 0^\circ$; (f) $\Gamma_1/cU_\infty = 1.0$, $Q/cU_\infty = -0.15$, $\alpha = 0^\circ$; (g) $\Gamma_1/cU_\infty = 1.0$, $Q/cU_\infty = -0.2$, $\alpha = 0^\circ$.

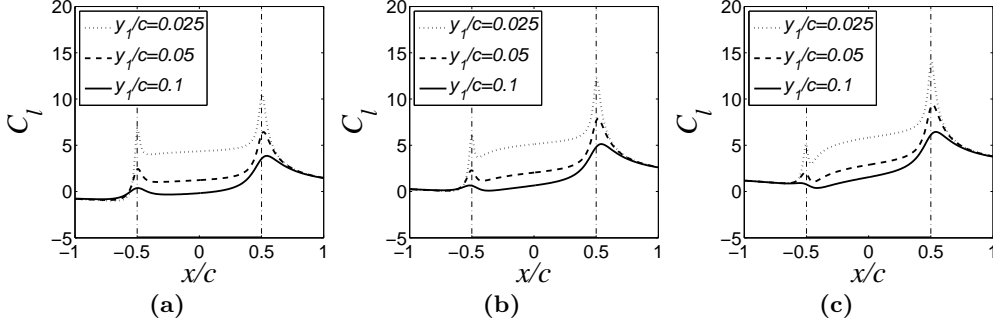


FIGURE 6. Lift coefficient C_l as a function of y/c for each x/c . $\Gamma_1/cU_\infty = 1.0$, $Q/cU_\infty = -0.1$ for all cases. (a) $\alpha = 0^\circ$; (b) $\alpha = 10^\circ$; (c) $\alpha = 20^\circ$.

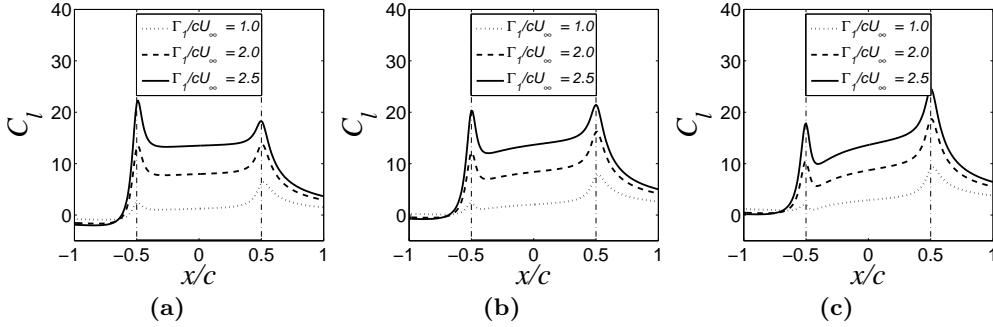


FIGURE 7. Lift Coefficient C_l as a function of Γ_1/cU_∞ for each x/c . $y/c = 0.05$, $Q/cU_\infty = -0.1$ for all cases. (a) $\alpha = 0^\circ$; (b) $\alpha = 10^\circ$; (c) $\alpha = 20^\circ$.

proaches the plate boundaries, the vortex-sink velocity approaches infinity because of its interactions with the singular point at the edge, which in return boosts the lift of the flat plate.

4.2. Effect of Vortex Strength (Γ_1/cU_∞)

By comparing the lift contours with different vortex strengths in Figure 5(a,d,e), it can be noticed that increasing vortex strength will increase the lift coefficient for all regions above the flat plate and in particular near the leading edge. As shown in Figure 7, the coefficient of lift varies as a function of x_1/c for different values of Γ_1/cU_∞ . It is verified that the increased strength of the leading edge vortex has a significant impact on improving the lift coefficient when the vortex-sink is above the flat plate. Furthermore, as is shown in all figures, especially in Figure 7(a), the increased vortex strength enhances the lift to such an extent in the region near the leading edge that the peak lift exceeds that of the trailing edge. However, by comparing the plots of different angles of attack it is clear that this strong lift enhancement near the leading edge might be reduced by increasing angle of attack.

4.3. Effect of Sink Strength (Q/cU_∞)

Figure 5(a,f,g) shows the lift coefficient contours with different sink strengths, from which not much variation could be observed. As further shown in Figure 8, the lift coefficient varies as a function of x_1/c for different values of Q/cU_∞ . Comparing the lift coefficients, it is found that as the strength of the sink increases there is a small increase in lift coefficient over a large region of x/c above the flat plate, specifically at the region near the trailing edge. However, the variations of lift coefficient with sink strength are still small

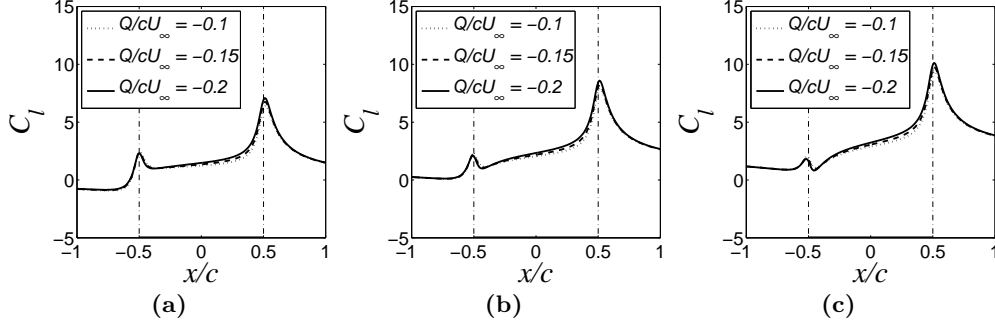


FIGURE 8. Lift Coefficient C_l as a function of Q/cU_∞ for each x/c . $y/c = 0.05$, $\Gamma_1/cU_\infty = 1.0$ for all cases. (a) $\alpha = 0^\circ$; (b) $\alpha = 10^\circ$; (c) $\alpha = 20^\circ$.

enough that they could be neglected. Therefore, we can conclude that the contribution of sink strength on lift is minor.

4.4. Effect of Angle of Attack (α)

As shown in Figure 5(a,b,c), and Figures (6,7,8), changing α does not cause significant variations in the results for most vortex-sink positions above the flat plate. It is therefore concluded that the presence of the vortex-sink makes the angle of attack a less effective factor for the lift coefficient (provided that the flow remains attached and the potential flow model assumptions are valid). However, as the vortex-sink is placed near the leading edge, an increased angle of attack apparently decreases the coefficient of lift as seen in Figures (6,7,8). In contrast, as the vortex-sink nears the trailing edge, an increased angle of attack enhances the coefficient of lift. This behavior of the C_l at the leading edge and trailing edge is due to the $\frac{a^2 e^{i\alpha}}{\zeta_1^2}$ term in Equation (3.12), which relates the vortex-sink location and angle of attack. Essentially, this indicates that a change of angle of attack will affect the vortex-sink velocity differently at either edge of the flat plate, and thus the vortex-sink velocity variation affect the lift coefficient through Equation (3.14) and Equation (3.15).

4.5. Summary for Lift Optimization

From the above analysis, the enhanced lift performance achieved by attaching a vortex-sink to a flat plate is verified. Areas near the leading edge and trailing edge close to the surface of the flat plate are found to be the locations for a significantly enhanced lift coefficient. In the direction along the flat plate, the best location for maximum lift should be the trailing edge in most cases; however, if the vortex strength is large enough, the maximum lift could be realized around the leading edge. Now, if the case of a flapping insect wing is considered, one might expect the location of the LEV to be related to optimal lift. However, for natural flight the vortex strength Γ_1/cU_∞ is experimentally evaluated to be around 1.0 (Bomphrey *et al.* (2005)). Around this magnitude of vortex strength, the results of this investigation show that the maximum lift is achieved near the trailing edge. Moreover, the natural trapped vortex center is not right at the leading edge but near the quarter chord of the airfoil as shown experimentally by Bomphrey *et al.* (2005). As shown in Figure 6,7, and 8, the quarter chord is the region where the flat plate would obtain some lift enhancement, but not the optimal lift. Therefore, we can conclude that the natural LEV is not placed at the position of maximized lift. Nevertheless, we hypothesize that the reason why insect flight stabilizes the vortex downstream of the leading edge might be related to the natural equilibrium and stability of the vortex which is discussed in the following sections. This is potentially an important concept for

flow control; since the natural vortex is generated at the leading edge, it should be much easier and faster to stabilize the vortex-sink in this region as opposed to near the trailing edge.

The results presented here show that the most effective ways of enhancing lift are increasing the vortex strength and placing the vortex close to the top surface and the two edges of the flat plate. The essence of this lift enhancement is attributed to the interaction between the vortex and the airfoil which creates positive lift on the flat plate while increasing the induced velocity of the vortex-sink due to its interaction with its image counterpart. This indicates that future control strategies could also be aimed at regulating the induced velocity of the vortex-sink in addition to only controlling the vortex location or the vortex strength. This means that there could be another alternative direction for future flow control applications: instead of stabilizing the vortex on a flat plate to obtain a steady lift enhancement, it is also possible to obtain a momentarily significant lift boost by manipulating the induced vortex velocity.

5. Unsteady Effects

In this section, the validity of this model is discussed by comparing the lift with previous experimental and theoretical results. One might be skeptical about using a steady state potential flow model to represent an unsteady flow; however, we argue that this model could be considered as the first approximation in unsteady flows. In fact, the primary objective of this study is to understand the role played by the vortex and span-wise flow in lift enhancement. Although the vortex-sink is motivated by flapping wing flights, the core of this study is more aimed at fixed wing flights flying at simple conditions such as cruising. We believe that by implementing modern flow control actuators, the lift performance of a manmade air vehicle could be significantly enhanced by properly placing a vortex-sink around the airfoil. Therefore, this simple 2D steady state potential flow model is considered to be adequate in studying the aerodynamics of the vortex-sink at this stage.

Moreover, for an unsteady flow, this model is to some extent representative of the flow pattern and thereby the lift optimization of vortex-sink locations should also provide insights into flow control strategies. The reason is explained below. As investigated experimentally by Dickinson *et al.* (1999) and numerically by Minotti (2002), the unsteady lift is computed at each time step of a flapping cycle. According to their studies, the overall unsteady lift is divided into three components based on different contributions, namely the translational lift (accounting for the potential flow force), rotational lift (accounting for the inertial force) and added mass (accounting for the transitional force). If the lift were to be computed for a flapping wing using this model, only the translational lift would be considered while the rotational lift and added mass term brought by unsteady motion being ignored. However, at each transient moment, the rotational lift and added mass terms should remain rather constant regardless of where the vortex-sink is located. The reason is explained here: the rotational lift could be interpreted as the force to maintain a rigid body rotation of the airfoil in the flow field, while the added mass term could be interpreted as the force due to angular acceleration and incoming flow acceleration. Apparently, the location of the vortex-sink has minor effect on these factors that determine the rotational lift and the added mass term. This means that the overall lift force calculation for each moment is not necessary in lift optimization, provided that the variations of vortex-sink location only affect the translational lift. Therefore, it is implied that the variation trend of the translational lift should be consistent with that of the overall lift for an unsteady flow.

Nevertheless, to demonstrate the performance of the translational lift calculation, here shows an example of flapping wing simulation using steady state model. The result is then compared with the overall lift by Minotti (2002) and experimental data by Dickinson *et al.* (1999) as shown in Figure 9. Basically, this simulation is implemented under the same condition as that of Minotti (2002)'s, which essentially simulated a flapping wing experiment done by Dickinson *et al.* (1999). Figure 9(a) shows the time variation of the angle of attack and incoming flow velocity, which defines the unsteady motion and the flow environment of the flat plate. By comparing the resultant lift in Figure 9(b), the best lift matching of the Pseudo-steady model with the unsteady model occurs at $0.5 - 1.75s$, $2.6 - 3.0s$, $4.0 - 5.0s$ and $6.2 - 6.6s$. Obviously as seen in Figure 9(a), $0.5 - 1.75s$ and $4.0 - 5.0s$ are the time intervals in which both the angle of attack and the incoming flow velocity remain relatively constant. This is due to the rotational lift and the added mass term approximating zero (shown in Figure 9(b)) which implies a steady state condition. Therefore, the Pseudo-steady model matches with the Unsteady model in this case. Moreover, during the period of $2.6 - 3.0s$ and $6.2 - 6.6s$ in which both the angle of attack and the incoming flow velocity are experiencing variations, the Pseudo-steady model also shows a good matching with the Unsteady model. This is because the effect of the varied α and U_∞ causes the rotational lift and the added mass term to be equivalent in magnitude and reverse in sign. Apparently, the rotational lift and added mass term cancel each other out and result in the overall unsteady lift being equal to the steady state lift. However, at the other time intervals with significant changes in α and U_∞ , there are several peaks that the steady state model is unable to capture; for example, $t = 0.25s$, $t = 2.3s$, $t = 3.3s$ and $t = 5.9s$. This indicates that if total lift force were to be resolved for flapping wings, unsteady lift terms should not be ignored.

Finally, it should be noted that another major unsteady effect, which is the trailing edge vortex shedding, is not considered in this paper either. Actually, this is the unsteady effect that has influence on the implementation of Kutta conditions. Nevertheless, Minotti (2002) has showed in his study that steady Kutta condition could be applied for potential flow model in unsteady flow by matching the overall lift force computed with experiment data as shown in Figure 9(b). Therefore, in the frame of this manuscript, further unsteady effects are ignored.

6. Conclusion

A vortex-sink pair attached to an airfoil is used as a simplified two-dimensional, incompressible and irrotational model of a vortex-sink in a quasi-steady flow. The attached vortex is presented by an irrotational vortex while the 3-D span-wise flow is loosely modeled by a sink in the direction normal to the plane. Basic flow behaviors and the non-dimensional parameters controlling the lift are identified and steady state Kutta conditions are considered for lift evaluation.

A detailed sensitivity analysis was conducted in order to optimize the lift coefficient based on vortex-sink locations, as well as to understand the effect of vortex-sink strength and angle of attack on the lift coefficient. It was found that the induced vortex-sink velocity close to the wall is related to the lift enhancement created by introducing a vortex near the flat plate. Therefore, the optimized positions for lift enhancement are those close to the flat plate surface in the proximity of the leading edge and trailing edge. It is further concluded that moving the vortex-sink pair towards the flat plate top surface and increasing the strength of the vortex are the most effective approaches to enhancing lift.

It is therefore inspired that high lift performance could also be achieved by moving

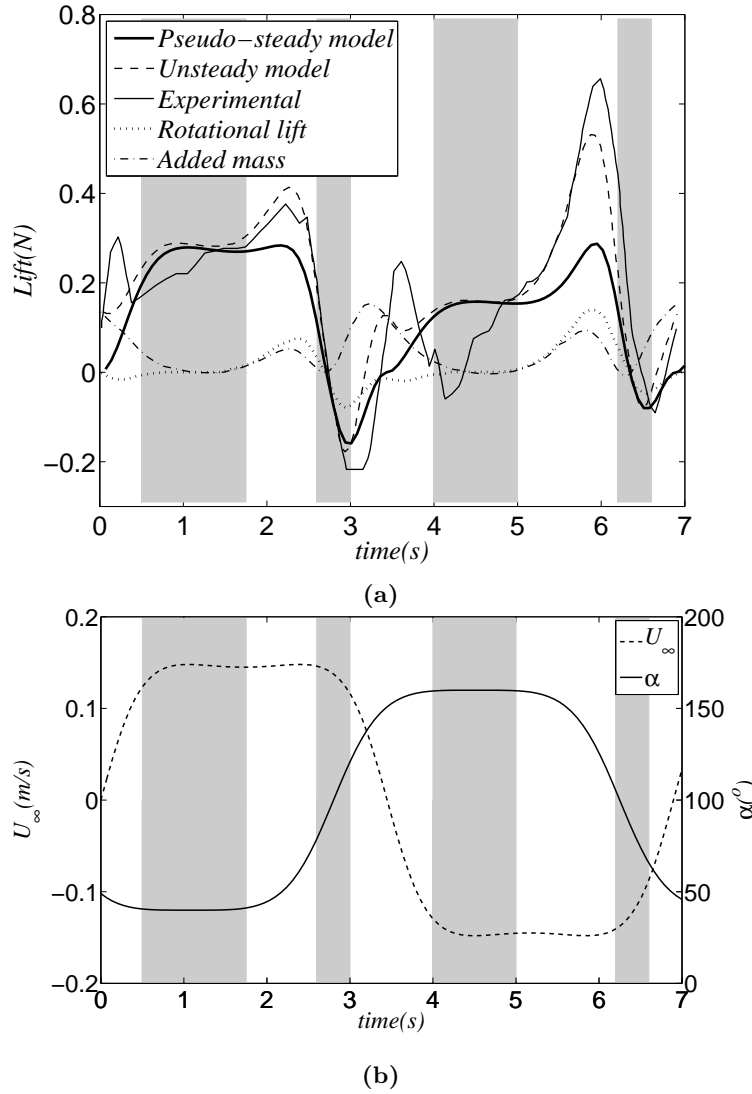


FIGURE 9. Lift comparison of a flapping wing experiment by Dickinson *et al.* (1999). (a) Comparison of lift variation with time. The Pseudo-steady model represents the lift computed from this model; the Unsteady model represents Minotti (2002)'s unsteady lift calculation; the Experimental is the lift measured by Dickinson *et al.* (1999) experimentally; Rotational lift and Added mass are the two unsteady lift components from Minotti (2002)'s unsteady model. The gray zones mark the regions where Pseudo-steady model shows good matching with the Unsteady model; (b) Time variations of α and U_∞ .

the vortex-sink. Rather than conventionally stabilizing the vortex to obtain a durable lift enhancement, it is also possible to realize a momentarily lift boost by actively controlling the motion of the vortex.

7. Acknowledgments

The authors would like to thank Christopher Davis and Shervin Shajiee for their preliminary work in developing the basics of the potential flow model as discussed in Reference Davis *et al.* (2009). The authors would like to thank an anonymous referee for his/her correcting comments on lift calculation. The authors would like to thank Matthiew Shields for his comments in improving the presentation of this manuscript.

REFERENCES

- ABLOWITZ, M. & FOKAS, A. 2003 *Complex Variables: Introduction and Applications*. Cambridge Univ. Press.
- BIRCH, J.M. & DICKINSON, M.H. 2001 Spanwise flow and the attachment of the leading edge vortex on insect wings. *Nature* **412**, 729–733.
- BOMPHELY, R.J., LAWSON, N.J., HARDING, N.J., TAYLOR, G.K. & THOMAS, A.L.R. 2005 The aerodynamics of *manduca sexta*: digital particle image velocimetry analysis of the leading-edge vortex. *J. Exp. Biology* **208**, 1079–1094.
- CHEN, S.H. & HO, C. M. 1987 Near wake of an unsteady symmetric airfoil. *Journal of Fluids and Structures* **1**, 151–164.
- CLEMENTS, R. R. 1973 An inviscid model of two-dimensional vortex shedding. *J. Fluid Mech.* **57**, 321–336.
- CORNISH, J.J. 1969 U.s. patent 3,480,234.
- CORTELEZZI, L. & LEONARD, A. 1993 Point vortex model of the unsteady separated flow past a semi-infinite plate with transverse motion. *Fluid Dynamics Research* **11**, 263–295.
- CRIGHTON, D.G. 1985 The kutta condition in unsteady flow. *Annual Review of Fluid Mechanics* **17**, 411–445.
- CROWDY, D. 2010 A new calculus for two-dimensional vortex dynamics. *Theor. Comput. Fluid Dyn.* **24**, 9–24.
- DAVIS, C.I.R., SHAJIEE, S. & MOHSENI, K. 2009 Lift enhancement in a flapping airfoil by an attached free vortex and sink. AIAA paper 2009-0390. 47th AIAA Aerospace Sciences Meeting and Exhibit, Orlando, FL.
- DICKINSON, M.H. & GOTZ, K.G. 1993 Unsteady aerodynamic performance of model wings at low reynolds numbers. *Journal of Experimental Biology* **174**, 45–64.
- DICKINSON, M.H., LEHMANN, F.O. & SANE, S.P. 1999 Wing rotation and the aerodynamic basis of insect flight. *Science* **284**, 1954–1960.
- ELLINGTON, C.P. 1984 The aerodynamics of hovering insect flight. iv. aerodynamic mechanisms. *Phil. Trans. R. Soc. Lond. B* **305**, 79–113.
- HUANG, M-K. & CHOW, C-Y. 1981 Trapping of a free vortex by joukowski airfoils. *AIAA* **20** (3).
- HUANG, M-K. & CHOW, C-Y. 1996 Stability of leading-edge vortex pair on a slender delta wing. *AIAA Journal* **34** (6).
- KANSO, E. & OSKOEI, B. G. 2008 Stability of a coupled body-vortex system. *J. Fluid Mech.* **600**, 77–94.
- KASPER, W. 1974 U.s. patent 3,831,885.
- KRISHNAN, G. & MOHSENI, K. 2009a Axisymmetric synthetic jets: An experimental and theoretical examination. *AIAA J.* **47** (10), 2273–2283.
- KRISHNAN, G. & MOHSENI, K. 2009b An experimental and analytical investigation of rectangular synthetic jets. *ASME J. Fluid Eng.* **131** (12).
- KUETHE, A.M. & CHOW, C.Y. 1998 *Foundations of Aerodynamics: Bases of Aerodynamic Design*. New York, NY: John Wiley and Sons, Inc.
- LIA, HAO, ELLINGTON, CHARLES P., KAWACHI, KEIJI, BERG, COEN VAN DEN & WILLMOTT, ALEXANDER P 1998 A computational fluid dynamic study of hawkmoth hovering. *The Journal of Experimental Biology* **201** (461-477).
- LIN, C. C. 1941 On the motion of vortices in two dimensions-i. existence of the kirchhoff-routh function. *Physics* **27**, 570–575.

- LOPEZ, OMAR D, MOSER, ROBER D, BRZOWSKI, DANIEL P. & GLEZER, ARI 2009 Aerodynamic performance of airfoils with tangential synthetic jet actuators close to the trailing edge. In *19th AIAA Computational Fluid Dynamics Conference*. san Antonio, TX.
- MICHELIN, S. & SMITH, S. G. LLEWELLYN 2009 An unsteady point vortex method for coupled fluid-solid problems. *Theor. Comput. Fluid Dyn.* **23**, 127–153.
- MILNE-THOMSON, L. M. 1958 *Theoretical Aerodynamics*. New York: Dover.
- MINOTTI, F. O. 2002 Unsteady two-dimensional theory of a flapping wing. *PHYSICAL REVIEW E* **66**, (051907) 1–10.
- MOURTOS, N.J. & BROOKS, M. 1996 Flow past a flat plate with a vortex/sink combination. *Journal of Applied Mechanics* **63**, 543–550.
- MUSE, JONATHAN A., KUTAY, ALI T., BRZOWSKI, DANIEL P., CULP, JOHN R., CALISE, ANTHONY J. & GLEZER, ARI 2008 Dynamic flight maneuvering using trapped vorticity flow control. In *46th AIAA Aerospace Sciences Meeting and Exhibit*, , vol. AIAA-2008-522. Reno, Nevada.
- POLING, D.R. & TELIONIS, D.P. 1987 The trailing edge of a pitching airfoil at high reduced frequency. *Journal of Fluid Engineering* **109**, 410–414.
- ROSSOW, V.J. 1978 Lift enhancement by an externally trapped vortex. *Journal of Aircraft* **15** (9), 618–625.
- SAFFMAN, P.G. & SHEFFIELD, J.S. 1977 Flow over a wing with an attached free vortex. *Studies in Applied Mathematics* **57**, 107–117.
- SMITH, S. G. LLEWELLYN 2011 How do singularities move in potential flow. *Physica D* **240**, 1644–1651.
- SWANTON, E., VANIER, B. & MOHSENI, K. 2008 Leading edge vortex stability in a flapping model hummingbird wing. AIAA paper 2008-3718. 38th AIAA Fluid Dynamics Conference and Exhibit, Seattle, OR.
- WILLMOTT, A.P., ELLINGTON, C.P. & THOMAS, A.L.R. 1997 Flow visualization and unsteady aerodynamics in the flight of the hawkmoth, *Manduca sexta*. *Phil. Trans. R. Soc. Lond. B* **352**, 303–316.